

Stochastic effects in mean-field dynamos

David Moss¹, Axel Brandenburg², Reza Tavakol³ and Ilkka Tuominen⁴

¹ Mathematics Department, The University, Manchester M13 9PL, UK

² NORDITA, Blegdamsvej 17, DK-2100 Copenhagen Ø, Denmark

³ School of Mathematical Sciences, Queen Mary and Westfield College, Mile End Rd, London E1 4NS, UK

⁴ Observatory and Astrophysics Laboratory, University of Helsinki, Tähtitorninmäki, SF-00130 Helsinki, Finland

Received February 11, accepted July 3, 1992

Abstract. Motivated by the observations that (i) the solar cycle is distinctly irregular on the long term, (ii) a proper treatment of the averaging processes of mean field theory yields stochastic terms that cannot be neglected in solar and stellar convection zones and (iii) the inclusion of parametrized nonlinearities in models with two spatial dimensions has not produced such irregular behaviour, we investigate the effects of various forms of noise on previously studied nonlinear $\alpha^2\omega$ dynamos in a sphere or a spherical shell. The study of the degree of fragility of the dynamo models in presence of stochastic perturbations is also interesting from a dynamical point of view. We investigate the consequences of perturbing solutions of both pure and mixed parity. In the former case we find that there can be quite pronounced deviations from the pure parity, and that these seem larger nearer to the relevant bifurcation. Effects are also stronger in a shell dynamo than in the full sphere. However, the magnetic period is relatively little changed in these examples. When a 2-torus solution (of mixed parity) is perturbed, the effects on the long period variations are much greater than on the short period, but even for quite strong perturbations the solutions do not leave the neighbourhood of the underlying attractor. We find our results to be robust, in that the precise nature of the noise term is qualitatively inconsequential; this is encouraging in view of the uncertainties present. We briefly contrast our results with those recently presented by Choudhuri for a model with one spatial dimension.

Key words: The Sun: magnetic fields – solar activity cycle – stars: magnetic fields – hydromagnetics – turbulence

1. Introduction

Mean field dynamo models have had varying degrees of success in reproducing the observed features of the solar dynamo. Kinematic models only require the solution of the dynamo equation (i.e. the induction equation with modified Ohm's law). Linear, kinematic models prescribe the large scale velocity field (commonly differential rotation only) and certain properties of the small scale velocity fields, and since these properties are ill-known for stellar convection zones the form of the differential rotation,

alpha effect and turbulent diffusivity is often chosen quite arbitrarily. These solutions are necessarily steady or strictly time harmonic.

Nonlinear quasi-kinematic models, in which an extra “quenching” term is introduced, representing the feedback of the Lorentz force on to the large or small scale motions, and fully nonlinear models including the simultaneous solution of the Navier Stokes equation, have also been studied, albeit much less intensively. Although in principle more complex behaviour is possible, the solutions found so far are again either singly periodic, or have at most two periods simultaneously present (e.g. Brandenburg et al 1989a,b).

In contrast, the solar cycle is distinctly irregular or noisy. The well known “11 year” cycle period for the sunspot number (22 year magnetic period) is only an average, and the durations of individual cycles vary in the range 9-13 years, with perhaps even larger exceptional variations. If the sunspot number is a measure of field strength, then the implication is that this too varies from cycle to cycle. It has been suggested that the marked nonlinearity of the solar dynamo might be the cause of these variations (Tavakol 1978). Certain simple “toy” nonlinear dynamo systems, when driven to very supercritical dynamo numbers, can exhibit behaviour that is reminiscent of the variation of sunspot numbers (e.g. Cattaneo et al. 1984), but this kind of behaviour has not been found so far in more “realistic” nonlinear dynamo models in two spatial dimensions. However, even these models are so simplified and parameterized that this is not a compelling argument against an important role for nonlinearity. In addition, it may be that the dynamo numbers attainable by these codes are not sufficiently supercritical.

A complementary approach, that has been little investigated so far, is to recognize that the usual ways of modelling processes occurring in the highly turbulent solar (or stellar) convection zone involve parameterizations arising from averaging processes. An intrinsic property of such processes is that they are “noisy”, and this aspect is lost in standard mean field models. Inclusion of such effects in the mean field formulation means that random forcing terms should be introduced into the dynamo equations (see, e.g., Hoyng 1987a,b). A somewhat different simple model with only one spatial dimension, in which the noise was assumed to modify the α coefficient of mean field theory, has been studied by Choudhuri (1992).

It should be emphasized here that nonlinearities will be present in turbulent convection zones, together with the cor-

Send offprint requests to: David Moss

responding attractors, prior to the introduction of noise. The natural theoretical framework would therefore be the combination “attractors plus noise”. It then is possible to investigate, for example, the “fragility” of solutions when noise is added: when so perturbed do they remain near to their original phase space trajectories or do they depart markedly from them, even wandering into basins of attraction of other attractors of the system? In nonlinear dissipative situations, the nature of the corresponding attractors directly determines the effectiveness of noise as a modifying influence on the solutions. More precisely, the effect of noise is expected to depend on the strength of the attractors of the system considered, with marked departures expected for weaker attractors. This could be especially important for systems with multiple attractors which possess complicated and intertwined basins of attraction. A somewhat similar situation was studied by Meinel & Brandenburg (1990) in a one dimensional model, in which two attractors were approached alternately because of the presence of a noise term in the equations.

In this paper we study some aspects of this problem, using a modification of the axisymmetric nonlinear kinematic dynamo code described in Brandenburg et al (1989a). We examine the response of selected regular nonlinear solutions to noise that is introduced in several different ways. We note Hoyng’s (1988) comment that “It is to be expected that models studying the effect of fluctuations ... will nevertheless appear in the literature, but the difficulty ... is clear: \mathbf{F} will be chosen essentially arbitrarily ...”. Nonetheless we feel that some insight into the general properties of noisy dynamos can be obtained even without a satisfactory formulation of the noise terms. Of course, this limitation of our work must be kept clearly in mind. Fortunately our results appear quite robust, in that the exact manner in which the noise is prescribed seems to have little qualitative effect on our results.

2. Equations solved

The standard mean field induction equation takes the form

$$\partial\langle\mathbf{B}\rangle/\partial t = \nabla \times (\langle\mathbf{u}\rangle \times \langle\mathbf{B}\rangle + \alpha\langle\mathbf{B}\rangle) - \nabla \times \eta_T \nabla \times \langle\mathbf{B}\rangle, \quad (1)$$

where the vectors $\langle\mathbf{u}\rangle$ and $\langle\mathbf{B}\rangle$ are to be interpreted as mean field averages and α and η_T are turbulent transport coefficients. We assume axisymmetry, so that $\langle\mathbf{B}\rangle = \nabla \times a\hat{\phi} + b\hat{\phi}$, and also that $\langle\mathbf{u}\rangle = \Omega \times \mathbf{r}$ (i.e. the large-scale velocity is a pure rotation); $\alpha = \alpha_0 \cos \theta / (1 + \langle\mathbf{B}\rangle^2)$, with $\alpha_0 = \text{constant}$ and $\eta_T = \text{constant}$. The solutions can be classified by the usual two parameters $C_\alpha = \alpha_0 R / \eta_T$, $C_\Omega = \Omega_0' R^2 / \eta_T$, where $\Omega_0' = \text{constant}$. R is the radius of the computational volume and $\Omega = \Omega_0' x$, where $x = r/R$.

To see how the noise term is formulated, we shall look briefly at the derivation of the mean field induction equation. The standard procedure is to write

$$\mathbf{B} = \langle\mathbf{B}\rangle + \mathbf{B}', \quad (2)$$

$$\mathbf{u} = \langle\mathbf{u}\rangle + \mathbf{u}', \quad (3)$$

where the averaging operator $\langle \rangle$ is defined below. The standard (i.e. not mean field) induction equation

$$\partial\mathbf{B}/\partial t = \nabla \times (\mathbf{u} \times \mathbf{B}) - \nabla \times \eta \nabla \times \mathbf{B}, \quad (4)$$

(here η is the normal, not turbulent, resistivity) is then averaged over a length or time scale that is assumed to be much greater than the corresponding scale for the turbulent motions and much less than the scale of the large scale structure. The formal result is

$$\partial\langle\mathbf{B}\rangle/\partial t = \nabla \times (\langle\mathbf{u}\rangle \times \langle\mathbf{B}\rangle + \langle\mathbf{u}' \times \mathbf{B}'\rangle) - \nabla \times \eta \nabla \times \langle\mathbf{B}\rangle + \mathbf{F}, \quad (5)$$

where \mathbf{F} is a function satisfying $\nabla \cdot \mathbf{F} = \mathbf{0}$, and so we can write $\mathbf{F} = \nabla \times \mathbf{f}$. Hoyng (1987b) argues that \mathbf{F} is a stochastic function that arises from the non-commutativity of the averaging operator, and is thus of order either l_c/L or t_c/T , according to the averaging process used, where l_c , t_c , L , T are small and large scales for the space and time variables. Eq. (5) is of Langevin type. It is conventional to neglect the term \mathbf{F} in Eq. (5), leading to Eq. (1), but in typical astrophysical applications l_c/L and t_c/T are not very small, and so it is not obvious that this approximation is fully justified.

For the special case of axisymmetric mean field dynamos an alternative approach is possible. Assuming again that Eq. (4) describes a state that is nonaxisymmetric on small scales only, the mean field averaging process can be performed with respect to the azimuthal (ϕ) coordinate. Now Eq. (5) is obtained without the term in \mathbf{F} , i.e. we get exactly Eq. (1), but it is now possible to consider α as containing a part that is noisy with respect to the meridional spatial coordinates (r, θ) and/or time.

In the remainder of this paper we are concerned with the mean field quantities only. We consider the formulation of Eq. (5) to be of wider application as it can be applied to both axisymmetric and nonaxisymmetric dynamos, but in order to provide continuity and comparison with the work of Choudhuri (1992), some of the computations were performed by stochastically perturbing α . Specifically, we set

$$\alpha = \alpha_0 \cos \theta \left[\frac{1}{1 + \langle\mathbf{B}\rangle^2} + f(r, \theta, t) \right], \quad (6)$$

We here distinguish two cases. We denote by Model 0 the very simple ansatz

$$f = f(t) = c(2r(t) - 1), \quad (7)$$

where $r(t)$ is a random number in the range [0,1], and c is a prescribed scale factor. In Model 1 we put $f = f(r, \theta, t)$, with

$$f = \sum_{i=1}^{n_c} c(2s_i - 1) \exp(-d_i^2/d_c^2). \quad (8)$$

$d_i^2 = (r \cos \theta - r_i \cos \theta_i)^2 + (r \sin \theta - r_i \sin \theta_i)^2$, where the (r_i, θ_i) are randomly chosen points, d_c is a correlation length, and the s_i are random numbers on [0, 1], all changed every τ_c .

In Model 3 an extra term $\nabla \times \mathbf{f}(r, \theta, t)$ is added to the right hand side of Eq. (1), where each component of $\mathbf{f}(r, \theta, t)$ is given by an expression of the form (8), but with an extra factor $(x-x_0)^2(1-x)^2 h(\theta)$, $x = r/R$, introduced to avoid possible inconsistent and troublesome behaviour near the grid boundaries where a and/or b vanish. (x_0 is the inner grid boundary, $x_0 = 0$ for computations in a full sphere.) $h(\theta) = \cos \theta$ for f_r and $\sin \theta$ for f_θ and f_ϕ . Note that in this case the maximum value of the modulus of \mathbf{f} is much less than c , but conversely there is always the possibility that the perturbation is relatively large where a or b are small within the computational grid. In the Model 1 and Model 3 computations, typically $n_c = 20$ ($n_c = 25$ by error in some Model 1 cases). The various models are briefly summarized in Table 1.

In practice we found very little qualitative difference between computations for Model 1 and Model 3, and so the results presented with one of these values can be taken as representative of those obtained with the other. The gross behaviour of our

Table 1. Summary of models for stochastic forcing

Model	Perturbation	Equations
0	$f(t)$	Eq. (6), Eq. (7)
1	$f(r, \theta, t)$	Eq. (6), Eq. (8)
3	$\mathbf{F} = \nabla \times \mathbf{f}(r, \theta, t)$	Eq. (5), Eq. (8)

solutions is described in terms of two parameters. If $E^{(A)}$ and $E^{(S)}$ are the energies in the parts of the magnetic field that are respectively antisymmetric and symmetric with respect to the equatorial plane, then $E = E^{(A)} + E^{(S)}$ is the total magnetic energy in $r \leq R$, and $P = (E^{(S)} - E^{(A)})/E$ is the overall parity. A0 and S0 denote axisymmetric ($m = 0$) pure parity solutions with $P = -1$ and $P = +1$ respectively. We measure nondimensional time, τ , in units of the global diffusion time R^2/η_T .

3. Results

We mostly studied $\alpha^2\omega$ dynamos with $C_\Omega = -10^4$. Calculations in the full sphere $0 \leq x \leq 1$ without noise show a variety of behaviour as C_α is increased, from the first bifurcation at $C_\alpha = 0.55$ to values greater than unity (Brandenburg et al. 1989b). In brief, the A0 mode is first excited. At $C_\alpha = 0.73$ the S0 mode is also excited, but it is at first unstable to perturbations of the opposite parity. In the range $0.79 \lesssim C_\alpha \lesssim 0.90$ both the pure parity modes are unstable, but there are one, two or even three (meta) stable mixed parity modes present for a given value of C_α . These solutions are limit cycles or 2-tori. For $C_\alpha \gtrsim 0.9$ only the S0 mode is stable. We did study one α^2 model with $C_\alpha = 10$ (Sect. 3.6). In this case both pure parity solutions are steady, and stable to axisymmetric perturbations. In this paper we use a spatial resolution of 21×41 meshpoints. The positions of the bifurcations are slightly different from those discussed in Brandenburg et al (1989a,b), where a higher resolution was used. Our results do not change significantly when the resolution is increased.

3.1. Perturbations of pure parity solutions

In this subsection we consider solutions with $C_\alpha = 1.0$. For Model 1 and Model 3 we considered perturbations only to stable solutions, since an unstable pure parity solution subject to a disturbance that contains a component of the opposite parity will inevitably evolve to the neighbourhood of the stable solution. In principle it is possible to apply Model 0 perturbations to an unstable solution, but we shall not present any such computations here as they show no new features.

We considered dynamos operating in the full sphere, $0 \leq x \leq 1$ and adopted standard values $\tau_c = 0.005$ and, for Models 1 and 3, $d_c = 0.20$. We first looked at the limit cycle solution with $P = +1$, $C_\alpha = 1$. For Model 0 the energy is modulated, but the parity P necessarily remains always $+1$, because here the noise is independent of the spatial coordinates. See the first panel of Fig. 1, where $c = 0.1$. For Models 1 and 3, the perturbations also modulate the parity. Qualitatively the effects of the perturbations in Models 1 and 3 are very similar, if the values of c are suitably adjusted. The variation of energy E and parity P for a typical run of Model 1 with $c = 0.1$ are shown in Fig. 1. Most of the time P is near $+1$, but there are occasional large excursions in P , and

also large modulations of the total energy E . In the last panel of Fig. 1 we show the power spectrum of $E(t)$. Note the peak at a frequency of 130, twice the frequency of the unperturbed magnetic cycle. We also compared Model 3 computations with $c = 1.0$ and $C_\alpha = 1.0$ and 1.2. The variation of $P(t)$ from the value $+1$ was typically twice as large when $C_\alpha = 1.0$ as when $C_\alpha = 1.2$, and the variations of $E(t)$ from the unperturbed oscillation were also larger for $C_\alpha = 1.0$.

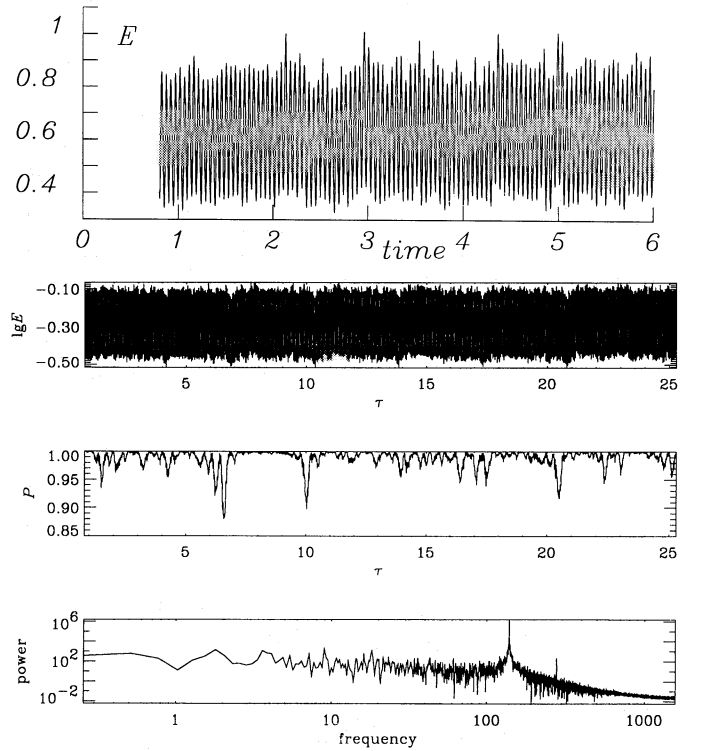


Fig. 1. Perturbations to limit cycle with $P = +1$, $C_\alpha = 1.0$, $C_\omega = -10^4$, $c = 0.1$. The first panel shows $E(t)$ for the Model 0 calculation. The remaining panels show $\log E(t)$, $P(t)$ and the power spectrum for E , for Model 1

All our calculations in a full sphere have $\tau_c = 0.005$. Trials with $\tau_c = 0.01$ in this case suggest that, for fixed values of the other parameters, effects are then somewhat more pronounced in that the excursions in P and E are larger. We use somewhat different parameters for calculations in a spherical shell, see Sect. 3.5.

3.2. Perturbations to a mixed parity limit cycle

We also examined the effects of perturbing the stable limit cycle of mixed parity, found when $C_\alpha = 0.79$. Again the computations are for the full sphere. For comparison, we show the results of runs for both Model 1 with $c = 0.1$ (Fig. 2) and Model 3 with $c = 1.0$ (Fig. 3). We would emphasize that the magnitude of the variations in the Model 1 computation would resemble more closely those of the Model 3 run if the value of c was reduced somewhat. For comparison, in the third panel of Fig. 3 we also show the unperturbed solution.

In addition we repeated both the Model 1 and Model 3 computations with $C_\alpha = 0.78$ and the other parameters unchanged. The fluctuations in both P and E were much smaller, and eventually P varied near the value -1 , which is the P -value of the unperturbed solution for this value of C_α .

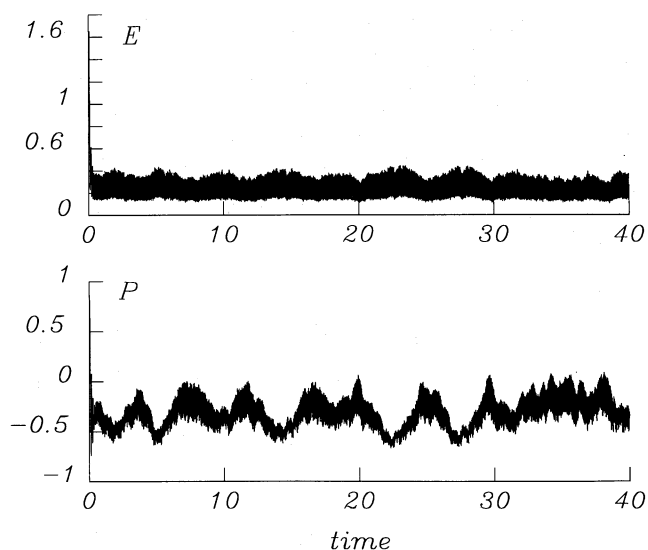


Fig. 2. Perturbations to the mixed parity limit cycle with $C_\alpha = 0.79$, $C_\omega = -10^4$, $c = 0.1$: $E(t)$ and $P(t)$ for Model 1

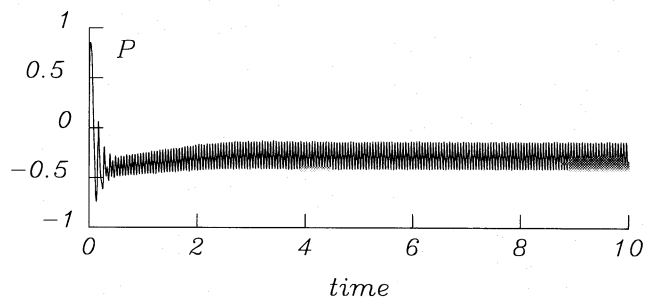
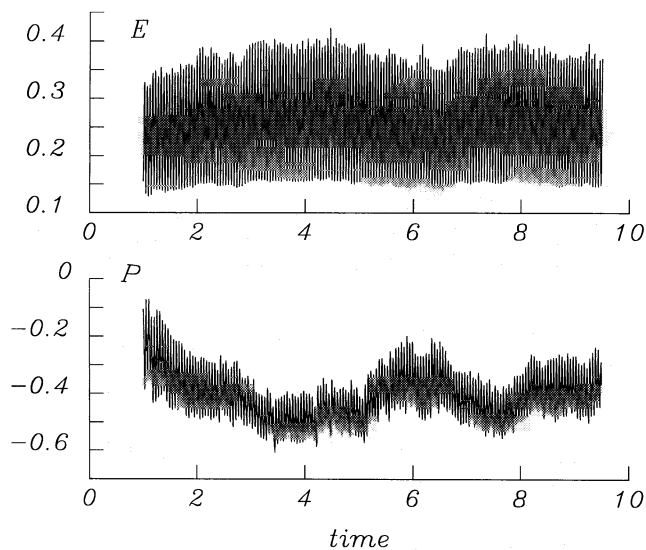


Fig. 3. Perturbations to the mixed parity limit cycle with $C_\alpha = 0.79$, $C_\omega = -10^4$: $E(t)$ and $P(t)$ for Model 3 (first and second panel), $c = 1.0$ and $P(t)$ for the unperturbed solution (third panel)

3.3. Perturbations to a torus solution

Next we look at the effect of perturbing a stable 2-torus solution, found when $C_\alpha = 0.81$. We performed Model 0, 1 and 3 calculations in the full sphere for this case. For suitably adjusted values of c we found that the overall differences in behaviour between these different cases were no larger than the differences between, say, two computations with Model 3 and different sets of random numbers. In Fig. 4 we present the results from a computation with Model 3 and $c = 1.0$. Note the strong modulation of the length of the “long” period, and of the overall energy variation of this period. When c was reduced to 0.5, similar modulations of the cycle length and energy maxima were found but were, of course, of smaller magnitude. For both of these cases the basic torus solution survives and is clearly visible through the noise. When the strength of the perturbation is increased to $c = 5.0$ this statement is no longer true, and the nature of the variations changes quite markedly. In particular the quasi-regular long period variations have more-or-less disappeared. This is especially true of the variation of $P(t)$, which appears now to be undergoing irregular, large departures from $P = -1$. The maximum variations of P seem approximately to coincide with episodes of minimum variation of $E(t)$, see Fig. 5.

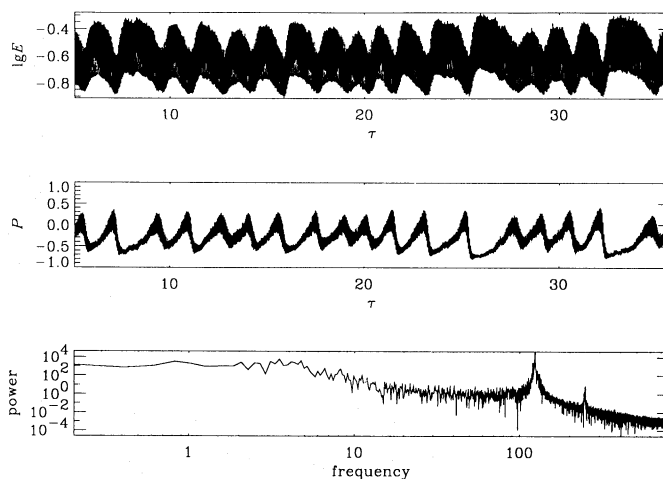


Fig. 4. Perturbations to the torus solution with $C_\alpha = 0.81$, $C_\omega = -10^4$, $c = 1.0$, Model 3: $\log E(t)$, $P(t)$ and power spectrum of $E(t)$

3.4. Multiple solutions

For $C_\alpha = 0.80$ there are three stable solutions: a pure parity $P = -1$ limit cycle, a mixed parity limit cycle with $P \approx 0.9$ and a mixed parity 2-torus solution. It might be expected that the different solutions might have different degree of fragility. We investigated the effect of noise on the two mixed parity solutions for the standard parameters $c = 1.0$ and $\tau_c = 0.005$, Model 3. There is no clear evidence that one of the two solutions is more fragile than the other. The E and P plots for the torus solution generally resemble those shown in Fig. 4, and those for the limit cycle are qualitatively similar to those in Fig. 3. We also looked at Poincaré maps showing intersections of the phase space trajectories of these solutions with arbitrary hyperplanes. The signatures of these two perturbed mixed parity solutions were quite similar (the torus is weak), but the mean positions of the intersections are slightly different. This result is perhaps

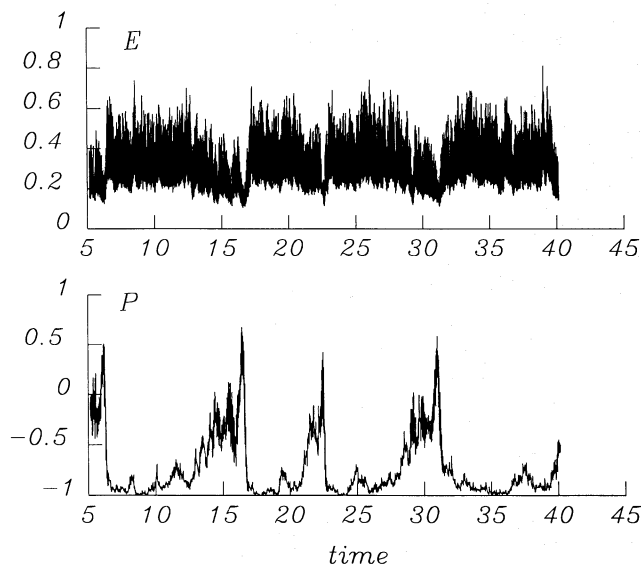


Fig. 5. Perturbations to the torus solution with $C_\alpha = 0.81$, $C_\omega = -10^4$, $c = 5.0$, Model 3: $\log E(t)$ and $P(t)$

somewhat surprising, because the mixed parity limit cycle solution exists only for a much smaller range of C_α than the 2-torus solution. Obviously, if we applied perturbations of much larger amplitude, then this situation might be altered. However, in such a case the perturbations may be already so strong that it would be hard to identify the solutions as being either a limit cycle or a 2-torus.

3.5. Effects in a shell dynamo

We also performed a few experiments with a shell dynamo, $x_0 \leq x \leq 1.0$, with a perfect electrical conductor boundary condition at $x = x_0 = 0.7$. Because of the reduced time and length scales in this case, we put $\tau_c = 0.002$, $d_c = 0.1$. Again taking $C_\omega = -10^4$, and starting from an arbitrary mixed parity configuration, we found unperturbed limit cycle solutions with very slowly varying parity in the range $0.8 \lesssim C_\alpha \lesssim 1.0$. This behaviour appears to be due to the structure of symmetric and antisymmetric solutions being much more similar in spherical shells than in spheres. At $C_\alpha = 0.81$, the unperturbed solution is evolving very slowly (time scale $\gg 10$ diffusion times) to a state with $P = +1$. When this solution is perturbed, the rate of evolution towards the $P = +1$ state is markedly accelerated. In Fig. 6 the original limit cycle is shown for $\tau \leq 2.0$, and also the effects of a Model 3 perturbation with $c = 100$, $d_c = 0.10$, $\tau_c = 0.002$. (Because of the geometrical weighting factors in the definition of f , when $x_0 = 0.7$ the effective value of c is reduced by a factor of about 10 compared to the calculations with $x_0 = 0$.) Although we did not investigate this point in detail for this model, both on theoretical grounds and from our previous experience we would expect the rate of evolution to $P = +1$ to depend on the distance of C_α from the bifurcation value. In Fig. 7 we show the results of a Model 3 disturbance to the stable solution with $P = -1$ at $C_\alpha = 0.85$, again with perturbation parameters $c = 100$, $d_c = 0.10$, $\tau_c = 0.002$. A run with $c = 50$ and different random numbers shows a similar pattern of behaviour, with $P \approx -0.97$ now being the maximum excursion from the unperturbed state. These experiments show episodes of strong variation of $P(t)$ from the

unperturbed value that are of similar nature to those found in the full sphere (cf. Fig. 1c), but their duration now seems much longer than in the previous example.

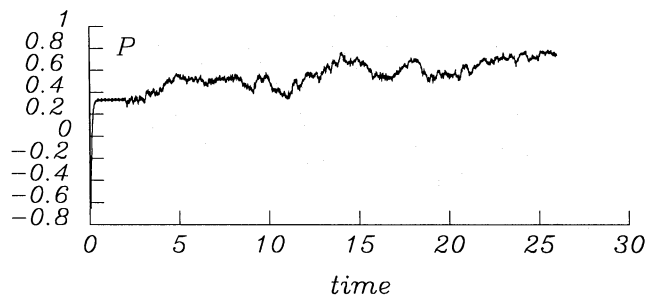


Fig. 6. Shell dynamo, $x_0 = 0.7$, Model 3, for $t < 0.2$ unperturbed solution and for $t > 0.2$ perturbations to mixed parity limit cycle with $C_\alpha = 0.81$, $C_\omega = -10^4$, $c = 100$: $P(t)$

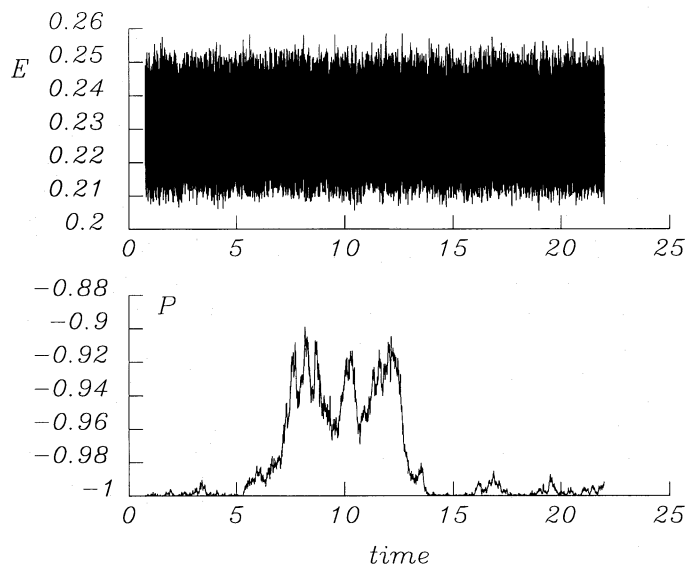


Fig. 7. Shell dynamo, $x_0 = 0.7$, Model 3, perturbations to $P = -1$ limit cycle with $C_\alpha = 0.85$, $C_\omega = -10^4$, $c = 100$: $E(t)$ and $P(t)$

3.6. An α^2 dynamo

We made a Model 1 perturbation to the stable $P = +1$ model with $C_\alpha = 10$ in the full sphere. Parameters were $c = 0.1$, $n_c = 20$, $\tau_c = 0.005$. This solution is shown in Fig. 8 for $1 \leq \tau \leq 20$, and can be compared with that shown in Fig. 1. Note, in particular, that the parity fluctuations for the α^2 model are much less ($O(0.003)$) than for the $\alpha^2\omega$ model ($O(0.1)$), inasmuch as it is valid to compare solutions at different distances from the relevant bifurcations. (We note that the α^2 solution with $P = +1$ is unstable to nonaxisymmetric perturbations, e.g. Rädler & Wiedemann (1989), in contrast to the $\alpha^2\omega$ models (Jennings et al 1990). However, there is no reason to anticipate that the response to our axisymmetric noise of the solution with $P = -1$, which is stable to such perturbations, would be qualitatively different.)

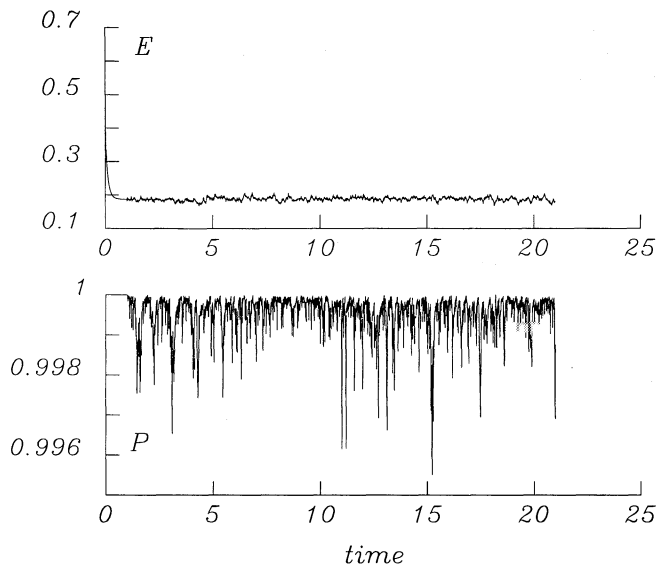


Fig. 8. α^2 dynamo in full sphere, Model 1, $C_\alpha = 10$, $c = 0.1$: $E(t)$ and $P(t)$

4. Discussion

The results outlined in Sect. 3 show clearly how noise with a correlation time that is a few percent of the basic period can modify the long term behaviour of a dynamo over timescales of many periods. For orientation, a correlation time $\tau_c = 0.002$ corresponds to about $1/20$ of the cycle period, which is about one year for the Sun. When we perturb a stable solution of pure parity, we find substantial departures from the pure parity state, occurring at irregular intervals and lasting for times that are long compared with both the correlation time and the basic cycle period. However changes to the individual cycle durations (quasi-periods) are small. This could be seen by looking in detail at small sections of the energy plot of Fig. 1, but is perhaps clearer in the power spectrum of $E(t)$. The basic oscillation frequency and its harmonic stand out clearly and cleanly. No other frequency is selected.

Our solutions over short time intervals are in some ways similar to those of Choudhuri (1992). In particular, the periods of his models also did not vary strongly in response to the imposed noise. Most of our results are for nonlinear $\alpha^2\omega$ dynamos, but the solitary α^2 model discussed in Sect. 3.5 does, however, suggest that our $\alpha^2\omega$ models may be more sensitive to stochastic perturbations than the α^2 . Compare, for example, Fig. 8 with Fig. 1. We note that Choudhuri found nonlinear $\alpha^2\omega$ models to be the *least* sensitive to stochastic perturbations. He did not present results for models that had been evolved for many diffusion times. Inspection of, for example, Fig. 7, demonstrates that behaviour during a short time interval can not necessarily be extrapolated for several diffusion times. Choudhuri found that nonlinearities suppressed the effects of noise. The solutions presented here are always limited in amplitude by the nonlinearity in α . Our dynamo numbers are only modestly supercritical, and it may be that the effects of noise are more strongly reduced by the nonlinearities in a more supercritical regime.

The effects of perturbing the mixed parity solutions are more noticeable. In principle, a wider range of behaviour might be anticipated, because when $C_\alpha \gtrsim 0.8$, there are two or three coex-

isting stable solutions, and so a fragile solution has the possibility of evolving to a nearby, more robust, attractor. However our admittedly limited experimentation did not provide any evidence for such behaviour, even for disturbances of larger magnitude than those reported on above. When $C_\alpha = 0.79$ (Fig. 2), the underlying limit cycle solution is unique, with $-0.5 \lesssim P \lesssim -0.2$. The perturbed solution can exhibit quite strong long period fluctuations in both P and E . When $C_\alpha = 0.80$ or 0.81 , the 2-torus is not the only stable attractor available to the system. However the basic solution survives the perturbations, but with marked effects on the long term behaviour. The short cycle period is again little affected – see the power spectrum of $E(t)$ in Fig. 4, where the cycle period and its harmonic are present as sharp peaks. By direct inspection of $E(t)$ we can estimate the maximum change of the short period to be of order 5%, and note that this is rarely attained. The signal from the long period (unperturbed frequency about 3.8) is almost indiscernible, as might be expected from an examination of the powerspectrum in Fig. 4.

From our limited evidence (Sect. 3.2), it is not easy to move a bifurcation, i.e. to kick an oscillator from one sort of behaviour (limit cycle, $P = -1$) into another (limit cycle, mixed parity), that becomes available to the unperturbed system at a slightly larger C_α value. Both in this case and for the pure parity limit cycle discussed in Sect. 3.1, the sensitivity of the solution seems to increase nearer to the bifurcation. This behaviour is expected on general grounds. Similarly it appears difficult to move a solution from the neighbourhood of one attractor to that of another unperturbed solution that exists at the same parameter values (Sect. 3.4).

To estimate the relative size of the perturbing terms, in the Model 3 calculation we can calculate, as functions of time, the spatial means of the absolute values of the three source terms occurring in the equation for the toroidal component of field, b . These terms are the α -effect, the differential rotation and the stochastic driving term. For the calculation with $c = 1.0$ discussed in Sect. 3.3 and presented in Fig. 4, we find that the mean stochastic term is nearly always substantially smaller than the mean α -effect term, which in turn is three orders of magnitude smaller than the differential rotation. Fig. 9 shows the relative sizes of the terms over an interval approximately the length of a long period of the solution. It should also be remembered that the α -effect and differential rotation vary only slowly in space, whereas the stochastic perturbation changes sign over small spatial scales. Note also that we have here an $\alpha^2\omega$ dynamo operating in a regime where the α term in the toroidal equation is to a good approximation negligible, and its neglect would not significantly change the solution (the $\alpha\omega$ approximation.) Thus the perturbation is genuinely “small”.

One motive for looking at the shell dynamo, $x_0 = 0.7$, was that the preference for one or the other of the pure parity states is only marginal, as evinced by the very slow evolution of $P(t)$ in the unperturbed system. The first bifurcations of the odd and even parity modes are at very similar values of C_α . Also, of course, the solar dynamo operates in a shell! Our result here is that the evolution to pure parity is accelerated by the presence of noise, at least at intermediate values of P , with a marked modulation of E and P . An interpretation of the sustained departure from the stable $P = -1$ solution apparent around $\tau = 10$ in Fig. 7 (comparable behaviour was not found in the full sphere calculations), is that because of the relatively weak evolution to the stable state found in this model, once a substantial departure from $P = -1$ occurs, relaxation back to

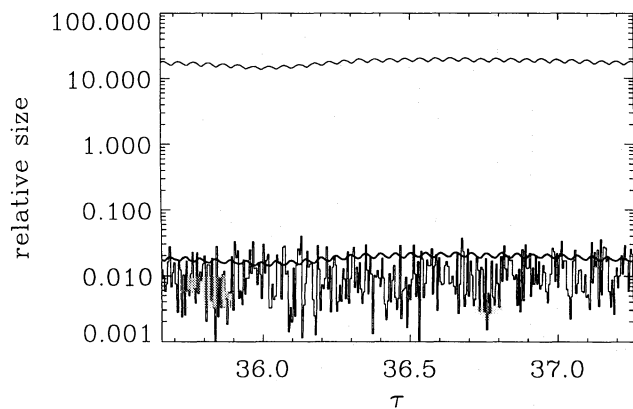


Fig. 9. The relative sizes of the spatial averages of the absolute values of the terms from the stochastic perturbation (lower thin curve), the α -effect (heavy curve) and the differential rotation (upper thin curve) in the toroidal field equation, for the calculation shown in Fig. 4

this state is slow.

In summary, our experiments do not show any evidence for marked fragility of the stable dynamo solutions. When stochastically perturbed, they remain near the basic attractor, even when there is another attractor that is in some sense not too distant in phase space. (We do not claim this to be a universal property, only that it is true of the solutions that we have investigated. It is quite likely that for other parameter values, corresponding to weaker attractors, this picture will change.) Nevertheless, in the case where there are two basic periods present, the longer of these can be strongly distorted, illustrating the cumulative effect of the stochastic forcing term. The “torus” solution with $c = 5.0$ (Sect. 3.3) seems to deviate considerably from the neighbourhood of its original attractor, but this is in some sense a strong perturbation. Clearly, other representations of stochasticity are possible. We are encouraged by the fact that our results do not depend strongly on the manner in which we introduce stochasticity to believe that the study of other models might lead to similar conclusions.

Our models are very distant from any realistic model of the solar dynamo. It is, however, perhaps a little disappointing that we find generally that the basic oscillation period is only weakly affected by the introduced stochasticity, although the energy variation from cycle to cycle does show stronger effects. Given that the length of the solar cycle routinely varies by about 20%, if these variations are to be explained by stochasticity, then the driving terms must be considerably larger than we have considered. However the long term behaviour of the 2-torus solution might just be reminiscent of the irregular spacing of the long term (Maunder-like) minima in the solar activity record. Certainly, we would not want to propose our perturbed torus model as a model for the occurrence of Maunder-type minima, but note in passing that if we just look at the variation of E above a threshold value of about 0.35 in Fig. 4, there might appear to be a slightly greater resemblance.

Acknowledgements. We thank Dr A.R. Choudhuri for a stimulating discussion and Dr A. Tworkowski for continuing discussions and suggestions. DM acknowledges the hospitality of the Observatory and Astrophysics Laboratory of the University of Helsinki and of NORDITA.

References

- Brandenburg, A., Krause, F., Meinel, R., Moss, D., Tuominen, I.: 1989a, *Astron. Astrophys.* **213**, 411
 Brandenburg, A., Tuominen, I., Moss, D.: 1989b, *Geophys. Astrophys. Fluid Dyn.* **49**, 129
 Cattaneo, F., Jones, C. A., Weiss, N. O.: 1984, *Geophys. Astrophys. Fluid Dyn.* **30**, 305
 Choudhuri, A.R.: 1992, *Astron. Astrophys.* **253**, 277
 Hoynig, P.: 1987a,b, *Astron. Astrophys.* **171**, 348; **171**, 357
 Hoynig, P.: 1988, *Astrophys. J.* **332**, 857
 Jennings, R., Brandenburg, A., Moss, D., Tuominen, I.: 1990, *Astron. Astrophys.* **230**, 463
 Meinel, R., Brandenburg, A.: 1990, *Astron. Astrophys.* **238**, 369
 Rädler, K.-H., Wiedemann, E.: 1989, *Geophys. Astrophys. Fluid Dyn.* **49**, 71
 Tavakol, R. K.: 1978, *Nature* **276**, 802